

Enhancing fidelity of virtual assembly by considering human factors

Wei Gao¹ · Xiao-Dong Shao¹ · Huan-Ling Liu¹

Received: 18 February 2015 / Accepted: 19 July 2015 / Published online: 1 August 2015
© Springer-Verlag London 2015

Abstract Virtual assembly (VA) provides a crucial opportunity to enhance product design and manufacturing efficiencies, but it still has no generic method to enable realistic behaviors during the assembly process. The real assembly process is strongly affected by the human factors and leaving the human aspect out of the assembly planning could result in incorrect or inefficient operations; however, this point is seriously neglected in the existing VA systems. This article simulates the human factors involved in the assembly process and analyzes the influence of the human factors on assembly performance on the basis of our previously presented physics-based assembly method, in which the assembling part is guided by the assembly force and the physics of the interaction is simulated. Assembly operations are simulated in a virtual environment, and the human factors including the visibility of an assembling part, posture, reachability, and fatigue of an operator are quantified. The new calculation methods of the estimated final position and the assembly force are presented to perform a more realistic assembly operation. This algorithm has been applied to a self-developed desktop virtual assembly prototype system. An example is illustrated, and the results show that this assembly method taking the human factors into account provides a realistic simulation of the assembly operations in virtual space and realizes a high consistence between virtual and real assembly process.

Keywords Virtual assembly · Assembly force · Human factors · Physics-based assembly

✉ Xiao-Dong Shao
13991138009@163.com

¹ Key Laboratory of Electronic Equipment Structure Design, Ministry of Education, Xidian University, Xian 710071, China

1 Introduction

Virtual assembly (VA) offers users an opportunity to assemble virtual representations of physical models through simulating realistic environment behavior and to validate assembly performance of products very early in the product development process. A well-designed assembly process can improve production efficiency and product quality, reduce cost, and shorten product's time to market. In manual assembly tasks, human involvement is very critical as it influences the feasibility, the cycle time, the working comfort, and safety of an operation. Nevertheless, building of physical prototypes increases development cycle time and cost. Thus, there has been a strong need for integrating human factors in the design and verification of industrial processes using simulation techniques [1]

To assist the user in performing an assembly task, some researchers have considered that the assembly process can be decomposed into two stages. Vance [2] divided the assembly task into a free movement phase and a fine positioning phase, and using independent techniques to implement each phase. Tching [3] decomposed a task into a guiding step which use geometries as virtual fixtures to position objects, and a functional step that use kinematic constraints to perform the assembly task while deactivating locally the collisions between objects.

We build upon previous work to propose the following classification of the assembly process: early assembly and later assembly. In the early assembly stage (see Fig. 1), the assembling part is driven by the user through the interactive device (such as virtual hand) to move from its initial position to the position that is close to the target position and collides with the base part. The main objective of early assembly is to ensure that the moving part does not collide with any other parts in virtual space. The technologies in this aspect have matured and have been utilized widely in engineering practice

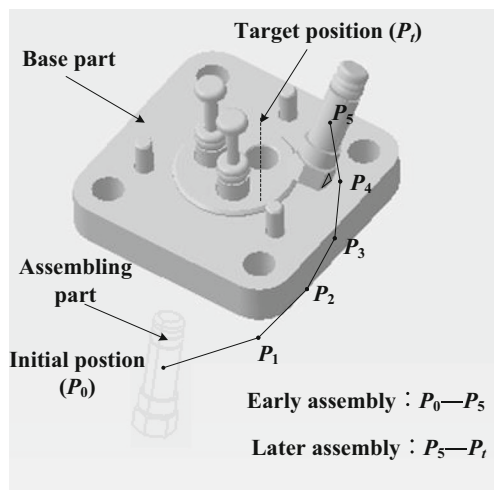


Fig. 1 Two stages of virtual assembly

[4]. In the later assembly stage, the assembling part is accurately positioned from the last position in the early assembly stage to the target position (see Fig. 1).

The assembly methods in later assembly stage have been studied for several decades and a vast amount of valuable achievements have been obtained. Generally, these methods can be categorized as either constraint-based modeling or physics-based modeling. Constraint-based methods use inter-part geometric constraints (typically predefined and imported) to determine relationships between components of an assembly [5]. Once constraints are defined and applied, a geometric constraint solver calculates the new and reduced degrees of freedom to enable precise relative positioning of parts, thus simplifying assembly, which do not take into account any physical interaction (part contacts, acceleration, colliding and gravitational forces, etc.) while simulating assembly. The key techniques of these methods are assembly relationship recognition, assembly constraint solution, and constrained motion under free and constrained spaces [6, 7]. Although constraint-based methods can rapidly and accurately position the assembly part in a virtual environment (VE), the complexity of geometric constraint recognition algorithms increases sharply with the growth of assembly complexity and the assembly process can not be simulated realistically.

Due to the problems related to constraint-based modeling, several approaches using physics-based modeling for virtual assembly have been proposed [8–10]. The physics-based modeling approach relies on simulating physical constraints for assembling parts in a virtual scene, which can significantly enhance the user's sense of immersion and interactivity. Physics-based algorithms simulate forces acting on parts in order to model realistic behavior and facilitate realistic interaction and dynamic response for assembly tasks. Such algorithms solve dynamic equations of the parts at each time step, based on their physical properties and the forces and torques that act upon them.

Based on these two categories of assembly methods, Seth [11, 12] proposed a method to demonstrate a combination of physics- and constraint-based behavior for virtual assembly, which takes advantage of physics-based methods to simulate dynamic behavior of colliding parts and geometric constraint modeling to support precise part manipulation. The challenge in this approach is that physics-based methods should be able to take into account the presence of a geometric constraint and the “hybrid solver” should be able to calculate part trajectories in such a way that both physical and geometric constraints are satisfied at any given point of time.

In general, while constraint-based approaches provide capabilities for precise part positioning in virtual environments, physics-based approaches, on the other hand, enable virtual mockups to behave as their physical counterparts. However, the existing assembly methods are unable to automatically guide the part to the final position and take into account the influence of human factors on assembly tasks. Holt et al. [13] propose that a key part of the planning process is the inclusion of the human expert in the planning and leaving the human aspect out of the assembly planning could result in incorrect or inefficient operations.

In our previous work, we reported on a method for assembly path planning based on force guidance in the later assembly stage, which can be used in the early design phase to validate an assembly process in simulating assembly conditions [14]. The main idea of the previously proposed assembly planning method is to use physics-based assembly methods to simulate the real assembly process and use Monte Carlo method to simulate the action of the human.

However, our previously proposed method can not quantify the human factors by theoretical calculation. The evaluation values of human factors are manually set by the user; thus, the evaluation results are sometimes inconsistent with the real world, which results in an inaccurate assembly process simulation and a low assembly efficiency. In order to quantify the human factors in real time and enhance the fidelity of assembly simulation, on the basis of our previous research, this article investigates the affects of the human factors on assembly performance and provides the quantitative calculation methods of the human factors including the visibility of an assembling part, posture, reachability, and fatigue of an operator. Furthermore, a new calculation method of the assembly force is presented to perform a more realistic assembly operation. The assembly force is calculated automatically according to the relative positions of the assembling part and the base part in real time. The assembling part is guided and positioned under the action of external forces. Thus, it does not need any haptic interactive devices during the assembly simulation process, which avoid the fuzziness and uncertainties of the input of devices [12].

The rest of the paper is organized as follows. In Section 2, some related researches on the assembly methods are

reviewed. Section 3 gives a basic idea of our previously presented assembly method and the quantitative calculation methods of human factors and assembly force. A test case of VA in a self-developed virtual assembly prototype system is presented in Section 4. A series of real-world experiments were carried out in Section 5 to test and verify the performance and capabilities of the proposed methods. Finally, Section 6 presents the conclusions of this work and defines the direction of future work.

2 Related work

The related work is divided into two sections: constraint-based assembly methods and physics-based assembly methods. Constraint-based methods apply constraints at the place of the assembly, which force objects to move along predefined paths. Physics-based methods use Newtonian physics to describe the motion of parts and simulate real-world physical properties, friction, and contact forces to parts in a virtual environment.

2.1 Constraint-based assembly methods

Jayaram and co-workers [15, 16] developed a representative VA system, Virtual Assembly Design Environment (VADE), which uses Pro/Toolkit to import assembly data (transformation matrices, geometric constraints, assembly hierarchy, etc.) from CAD to perform assembly operations in a virtual environment. Predefined geometric constraints are activated to simulate constrained motion when parts approach mutual proximity. Parts are then snapped to their final position to complete the assembly task. Similar research has been conducted by Wan et al. [17] in creating a Multi-Modal Immersive Virtual Assembly System (MIVAS). MIVAS used constraints for simulating part behavior in a virtual environment and used Pro/Toolkit for importing CAD geometry and predefined geometric constraints from Pro/Engineer CAD software.

Tching et al. [3, 5] proposed a method that uses both kinematic constraints and virtual guiding fixtures to help the user to perform the assembly of CAD objects, which allow the direct use of CAD data in the virtual environment by introducing the concept of virtual constraint guidance (VCG). The VCG method relies on virtual fixtures to guide the moving object to a specific position. VCG assists the user in precisely positioning the CAD model into the assembly. Marcelino et al. [18] developed a geometric constraint manager to support interactive assembly and maintenance tasks training using virtual prototypes. The constraint manager was capable of validating existing constraints, determining broken constraints, enforcing existing constraints, solving constrained motion, and recognizing new constraints

A CAD-linked virtual assembly environment was developed by Wang et al. [19], which utilized constraint-based modeling for assembly. With this framework, assembly constraint information can be feasibly integrated into the virtual assembly application with much less effort. Zhong et al. [20] incorporated constraints into the VE for acquiring precise constraint-based manipulations and derive allowable motions represented as a mathematical matrix from constraints.

Yang et al. [7] used constraint-based modeling for assembly path planning and analysis. Assembly tree, geometric data of parts, and predefined constraint elements could be imported from parametric CAD systems using a special data converter. Real time and interactively constraint recognition, confirmation, and motion navigation according to the assembly constraints, assembly levels, position, and orientation of parts in virtual space were performed to position parts accurately by satisfying all of the constraints. These capabilities were applied to the integrated virtual assembly environment (IVAE) system.

Zhang et al. [21] studied movement navigation based on geometry constraint recognition. With constraint-based DOF analysis, the assembly constraint hierarchical model is constructed and the system's constraints are built dynamically. The accurate locating of parts can be realized, and the realistic assembly operation process can be simulated. All objects in the VE can be located reasonably by movement navigation of constraints. Wang et al. [22] presented an enhanced constrained motion methodology to simulate multiple constraints used in assembly operations by considering three special cases, based on an analysis of axial and planar constraints used in assembly designs.

In 2007, Liu and Tan et al. [6] explored and develops a constrained behavior manager (CBM) for interactive assembly in a VE. CBM takes charge of assembly relationship recognition, assembly constrain solution, and constrained motion during the VA process. The key techniques employed in the constraint manager are direct interaction, automatic constraint recognition, constrain satisfaction, and constrained motion.

2.2 Physics-based assembly methods

Gupta and co-workers [23] made an early attempt at implementing physics-based modeling for simulating assembly behavior and developed a desktop-based system called Virtual Environment for Design for Assembly (VEDA), but this system is limited to 2D models. Coutee et al. [24, 25] utilized a similar approach relying on collision detection and physics computations for assembly to create a desktop-based virtual assembly system called Haptic Integrated Dis/Re-assembly Analysis (HIDRA). This system had problems handling non-convex CAD geometry, and thus, is only suitable for simulating assembly operations among simple primitive-based models. Fröhlich et al. [8] developed an interactive VA

system using physics-based modeling. The system used a responsive workbench for simulating bench assembly scenarios.

In 2007, Garbaya and Zaldivar-Colado [26] created a physics-based virtual assembly environment focusing on mechanical part assembly to address the problem of part-to-part contacts during the mating phase of an assembly operation. Contact force sensations were calculated by making their intensity dependent on the depth of penetration. In 2009, Garbaya and Zaldivar-Colado [27] focused on modeling the dynamic behavior of mechanical parts during the execution of virtual assembly operation. The concept of spring-damper model was adopted to preclude the interpenetration of parts during the mating phase, and the concept of “visual dynamic behavior” representing the manipulation of real parts was developed.

Kim and Vance [28] investigated several collision detection and part behavior algorithms to support the physics-based modeling of virtual manual assembly tasks. Wang et al. [29] discussed the benefits and limitations of physically based modeling in virtual environments. The mass properties of the assembly models are extracted from the CAD system while the design models are transferred from the CAD system to the virtual assembly environment. They discovered that certain presentations of gravitational acceleration needs to be scaled down to achieve maximum realistic feeling in the fully immersed virtual environment.

Lim [30] investigated assembly performance in the virtual environment using physics-based interactions. A kinematic evaluation of task performance for peg-in-hole manipulation based on geometric and force conditions is studied. Howard et al. [31] investigated the feasibility of an affordable haptic desktop system for evaluating assembly operations. This application combines several software packages including VR Juggler, OPAL/ODE, OpenHaptics™, and OpenGL/GLM to explore the benefits and limitations of combining physically based modeling with haptic force feedback.

In 2006, Seth et al. [32] developed a low-cost VR application that can provide dual-handed force feedback and realistic simulation of part behavior among complex CAD models while performing assembly tasks in virtual environments. This application, called System for Haptic Assembly and Realistic Prototyping (SHARP), used physically based modeling for simulating realistic part-to-part and hand-to-part interactions in virtual environments and allowed users to simultaneously manipulate and orient CAD models to simulate dual-handed assembly operations. In SHARP, realistic object behavior modeling is implemented using the Voxmap Point Shell (VPS) [33] software from Boeing Corporation. Using VR Juggler [34] as an application platform, the system could operate on different VR systems configurations including low-cost desktop configurations.

In 2010, Seth et al. [11, 12] attempted to demonstrate a combination of physics-based and constraint-based behavior

for virtual assembly where both physical and geometric constraints are created and deleted at run time. A solution to low clearance assembly was provided by utilizing B-Rep data representation of CAD models for accurate collision/physics results. These techniques are demonstrated in the SHARP software. Combining physics- and constraint-based techniques and operating on accurate B-rep data, SHARP can assemble parts with 0.001 % clearance and can detect collisions with an accuracy of 0.0001 mm.

3 Methodology

In this section, at first, our previously presented assembly method based on force guidance is reviewed. Then, the human factors are classified and each influencing factor is quantitatively calculated. Finally, the new calculation methods of the estimated final position and the assembly force are proposed to enhance the fidelity of the assembly operations.

3.1 Assembly method based on force guidance

The basic idea of our previously proposed assembly method is shown in Fig. 2. At first, the later assembly process is divided into multiple simulation steps. At step i , the external forces and moments exerted on the assembling part are calculated. The assembly force and assembly torque, applied by the user, are simulated by considering human factors. Once a collision is detected, the contact force is calculated. Then, the dynamic equations of the position, attitude, external forces, and moments are established automatically. The manipulated part is dynamic in nature, and its motion is subject to physics laws,

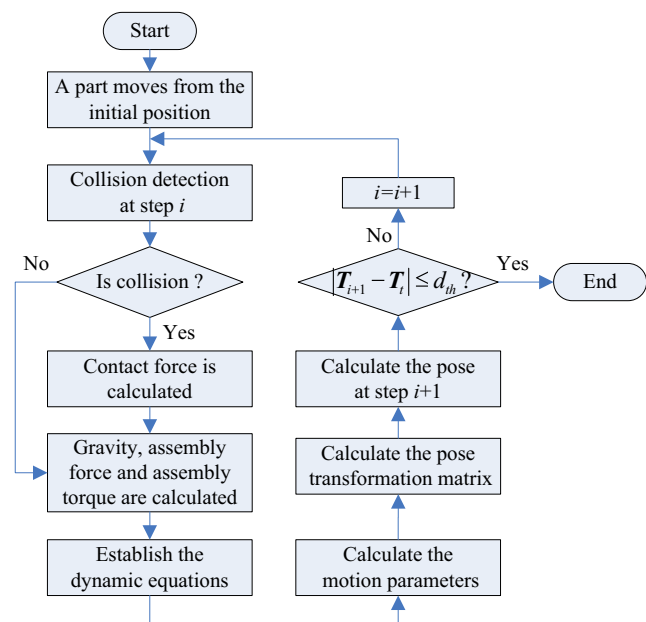


Fig. 2 The basic idea of assembly method based on force guidance

more specifically, rigid body dynamics. That is, given the dynamic state of a part at step i , its motion must satisfy Newton-Euler equations (see [14]). Finally, we will find the solution of the equations to obtain the part’s acceleration and angular acceleration and substituting them into the kinematics equations to calculate the displacement, rotation angle, and pose transformation matrix of the assembling part from step i to $i+1$, and then the position and attitude of the assembling part at step $i+1$ are calculated. If the distance between the part’s position at step $i+1$ (denoted by T_{i+1}) and final position (denoted by T_i) is less than the threshold (denoted by d_{th}), the assembly is completed. Otherwise, $i=i+1$ and the above steps are executed again.

With this method, the system automatically performs the following tasks at each simulation moment: (a) calculate the external forces and torques that act upon the assembling part, (b) solve the dynamic equations to obtain the motion parameters, and (c) find the position and attitude of the part at the next moment. Thus, it is a quite automatic assembly path planning method.

3.2 Human factors

In this section, we discuss the human factors involved in the assembly process, including the visual factor, the comfort factor, and the fatigue factor, and how to quantify these factors for each assembly operation.

3.2.1 Visual factor

The real-world assembly tasks have already shown that viewing perspective causes uncertainties during the assembly process and affects the task completion time and the difficulty of assembly operations [35]. In our method, the visual factor refers to the factor that has impacts on the positioning of the assembling part and the act of external forces, due to visibility of the assembly operation and eye sight direction of assembly operator.

We refer to the method presented by Enomoto et al. [36] to estimate the visibility of the assembly operation. V is defined as the estimation of the visibility of the assembly operation which is calculated as follows:

$$V = \frac{V_a}{V_b} \quad (V_b \neq 0) \tag{1}$$

Where, V_a is the number of pixels of the visible parts of the assembling part. V_b is the number of pixels of the assembling part. When V_a is calculated, all previously assembled parts and the assembling part are displayed in the assembly model. When V_b is calculated, only the assembling part is displayed and other parts are hidden. From Eq. (1), if there is no obstacle part to hide the assembling part, visibility estimation is 1. If

the assembling part is completely hidden by preassembled parts, visibility estimation is 0.

The eye sight direction is defined as the vector directing from eyes of an operator to the assembling part. The estimation of eye sight direction is determined by the angle between eye sight direction of the operator and the motion vector of the assembling part (denoted by Ang , $0 \leq Ang \leq 180$). It is assumed that Ang in the range from 30 to 45° is most preferable (estimation is 1) and the estimation decreases over 45° [36]. The estimation of a eye sight direction is denoted by f , which is derived by the function shown in Fig. 3. Then, the vision influencing coefficient η in our previous research [14], which represents the influence of the visual factor on assembly operation, is derived as follows:

$$\eta = 1 - Vf \tag{2}$$

From Eq. (2), it can be seen that η is not independent from the visibility estimation V . This is because the evaluation of the eye sight direction would be useless if the assembly area is completely invisible.

3.2.2 Comfort factor

The comfort factor is defined as the factor that is related to working comfort and affects the manipulation of parts during the assembly process. It is determined by the posture of human and effort required for orientating and positioning the assembling part. The comfort coefficient λ_c in [14], which indicates the comfort degree of the assembly operation, is quantified by the estimation of reachability of the operation and glance load to the operator’s neck.

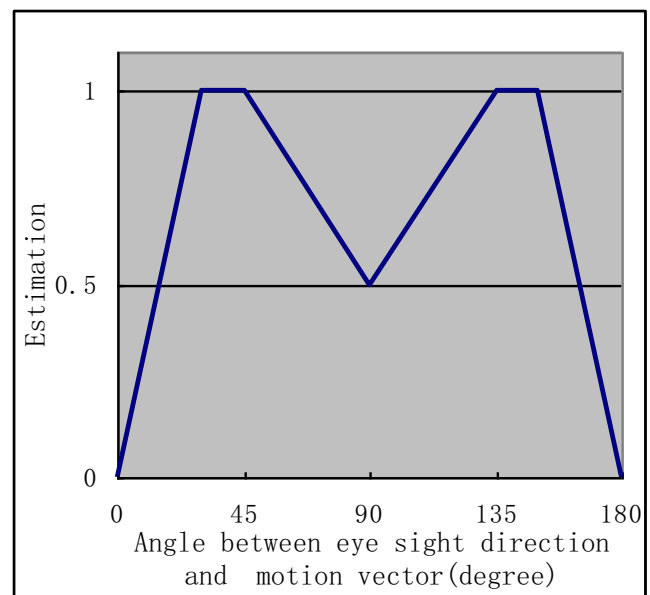


Fig. 3 Estimation of eye sight direction

The distance from the operator’s shoulder to the center of the assembling part is used to estimate the reachability of the operator. The estimation of reachability against distance from the operator’s shoulder to the center of the part is denoted by r , which is derived by the function shown in Fig. 4. It is easy to reach and manage the assembling part until distance D_1 . From D_1 to D_2 , it is possible to reach for the operator, but the difficulty increases with the increase of distance. From D_2 to D_3 , much effort is required for the operator to bend forward in order to manage the assembling part. It is impossible for the operator to reach with any posture when the distance is over D_3 .

In Fig. 4, D_i ($i=1, 2, 3$) is derived as $D_1=0.85l$, $D_2=0.39h$, and $D_3=0.68h$, where l is the length of the operator’s arm and h is the height of the operator. These parameters are referenced from [36] and are obtained empirically by testing different values until stable and smooth dynamic behavior of the virtual part is obtained.

Glance affects load to the neck of an operator. If the glance is looking up, it loads to the neck of the operator and increases the difficulty of assembly, which should be avoided. The glance is estimated by the angle between eye sight direction of the operator and the plane of the operator’s body (denoted by Anp , $0 \leq Anp \leq 180$). $Anp < 90$ means the glance is looking down, otherwise, it is looking up. According to the practical experience, it is reasonable to assume that Anp in the range from 30 to 90 ° is most preferable (estimation is 1) and the estimation decreases over 90 °, because looking up makes the operator feel uncomfortable. The estimation of glance is denoted by g , which is derived by the function shown in Fig. 5.

Then, the comfort coefficient λ_c in [14] is derived as follows:

$$\lambda_c = 1 - \frac{r + g}{2} V \tag{3}$$

In Eq. (3), it is assumed that λ_c is not independent from visibility estimation V with the same reason as previously

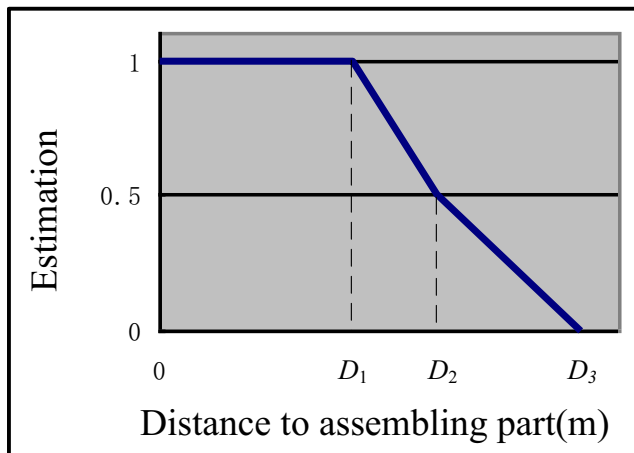


Fig. 4 Estimation of reachability

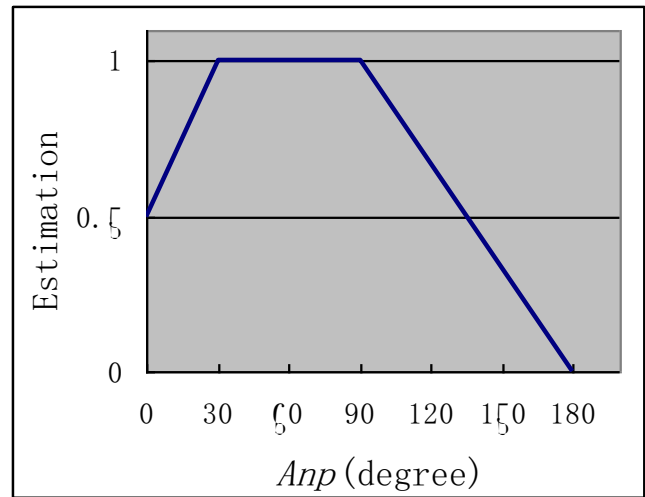


Fig. 5 Estimation of glance

described in Eq. (2). The maximum estimation of λ_c is 1 and the minimum score is 0. From Eq. (3), if product design conforms to ergonomics and the assembly task can be easily managed, λ_c is small. Otherwise, λ_c is relatively large, which means that the assembly performance should be improved in some aspects, such as reachability and glance.

3.2.3 Fatigue factor

The fatigue factor is defined as the affect of working time and workload on human performance, which indicates energy expenditure of the operator for manual operation. We use the energy consumption equation (see Eq. 4) given in [37] to calculate the energy consumption of the operator. For energy consumption, Institute of Health of Chinese Academy of Medical Sciences studies the relation between working time and energy consumption for representative 262 kinds occupation in China. The conclusion is the limitation value of energy consumption should be from 1400 to 1600 kcal in a working day (8 h)[37].

$$A = \left(F \cdot H_n + \frac{F \cdot L}{9} + \frac{F \cdot H_0}{2} \right) \cdot K \cdot n \tag{4}$$

where

- A Amount of work (J)
- F Assembly force (N)
- H_n The distance in which the object is lifted (m)
- H_0 The distance in which the object is lowered (m)
- L The distance in which the object is moved horizontally (m)
- K Coefficient (biomechanical criterion) characterizing moving individual sections of the body and equal to 6
- n Number of equal technological cycles

The influence of human factors on the assembly task is simulated by incorporating the human factors into the calculation of external forces in Monte Carlo method and this will be explained in detail in Section 3.3.

3.3 Calculation of assembly force

The assembly force is applied by the operator. It plays a major role in the guidance of the assembling part. According to the motion state of the assembling part, at each simulation step i , the assembly force can be categorized into two types: exerted on freely moving parts (denoted by F_{AFi}) and exerted on colliding parts (denoted by F_{ACi}).

3.3.1 Assembly force exerted on freely moving parts (F_{AFi})

For the real-world assembly task, in order to accurately guide a freely moving part (do not collide with any other parts in the scene) to its final position, the ideal assembly force should point from the part’s current position to the final position. However, as the influences of human factors, it is difficult to maintain the assembly force in that direction. As the moving part approaches the final position, the operator will continuously adjust the direction of assembly force for the purpose of reducing manual operation error. To enhance the fidelity of assembly in virtual environment, this paper takes the affect of human factors on the calculation of assembly force into account.

The direction of F_{AFi} is calculated by a probability method. At first, the estimated final position of the assembling part at time $i + 1$ (denoted by \mathbf{T}'_{i+1}) is calculated by the Monte Carlo method. Then, the assembly force is set up to point from the part’s position at step i (denoted by $T_i, T_i=(x_i, y_i, z_i)$) to \mathbf{T}'_{i+1} (see Fig. 6). \mathbf{T}'_{i+1} is calculated by Eq. (5).

$$\mathbf{T}'_{i+1} = \mathbf{T}_i + \frac{\lambda_c}{\Psi_c} \mathbf{T}_{i-1} + \mathbf{E}_i \tag{5}$$

where, $T_i=(x_i, y_i, z_i)$, $\mathbf{T}_{i-1}=(c_1(x_i-x_i), c_2(y_i-y_i), c_3(z_i-z_i))$, c_1, c_2 , and c_3 are all random numbers obeying uniform distribution in

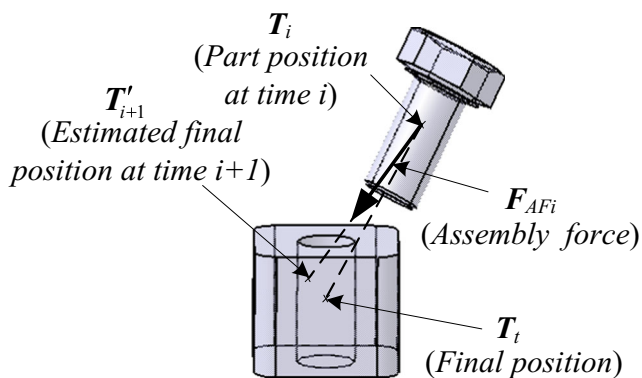


Fig. 6 The direction of F_{AFi}

the interval $[0, 1]$. Ψ_c is defined as the fatigue coefficient. $\frac{\lambda_c}{\Psi_c} \mathbf{T}_{i-1}$ represents the positioning errors caused by the comfort factor and the fatigue factor. Ψ_c is related to the duration of assembly tasks and is calculated by Eq. (6).

$$\Psi_c = \frac{1600-A}{1600} \quad 0 \leq A \leq 1600 \tag{6}$$

where, A is the amount of work and is calculated by Eq. 4. The calculation method of E_i , which is called the vision influencing matrix and represents the positioning errors caused by viewing perspective, has been discussed in detail in [14].

The magnitude of F_{AFi} is calculated by considering the fatigue factor (see Eq. (7)), because energy expenditure of the operator will affect the manipulation of parts and the act of assembly force.

$$F_{AFi} = \kappa \cdot \Psi_c \cdot D_i \tag{7}$$

where, $D_i = \sqrt{(x_i-x'_{i+1})^2 + (y_i-y'_{i+1})^2 + (z_i-z'_{i+1})^2}$ represents the distance between T_i and \mathbf{T}'_{i+1} and κ is called the assembly force coefficient and its calculation method is given in [14].

3.3.2 Assembly force exerted on colliding parts (F_{ACi})

The calculation method of F_{ACi} is similar to that of F_{AFi} . At first, \mathbf{T}'_{i+1} is calculated by Eq. (5). The vector from T_i to \mathbf{T}'_{i+1} is denoted by $\overrightarrow{T_i \mathbf{T}'_{i+1}}$. Then, the direction of F_{ACi} (denoted

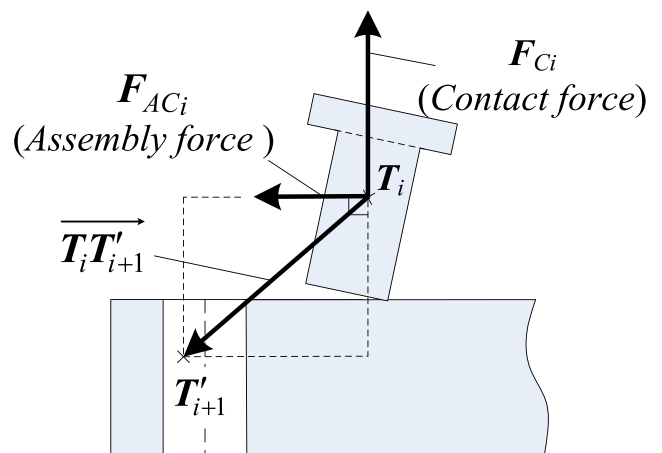


Fig. 7 The direction of F_{ACi}

by \vec{F}_{ACi} , see Fig. 7) is perpendicular to the direction of contact force and calculated by:

$$\vec{F}_{ACi} = \vec{T}_i \vec{T}'_{i+1} - \frac{\vec{T}_i \vec{T}'_{i+1} \cdot \vec{F}_{Ci}}{|\vec{F}_{Ci}|} \cdot \frac{\vec{F}_{Ci}}{|\vec{F}_{Ci}|}$$

where F_{Ci} is the contact force and its calculation method refers to [14]. The role of F_{ACi} is to overcome the friction (denoted by f) and navigate the part to the final position. The magnitude of F_{ACi} is proportional to $|\vec{F}_{ACi}|$ and is affected by the fatigue factor (see Eq. (8)).

$$F_{ACi} = \kappa \cdot \Psi_c \cdot |\vec{F}_{ACi}| + f \tag{8}$$

4 Assembly example

Supported by the proposed assembly method, a self-developed desktop virtual design platform (see Fig. 8) has been developed. A case study for the assembly of hydraulic cylinder consisting of four subassemblies is used here to test and verify the performance and capabilities of the proposed system for supporting assembly path planning and human factors analysis. Figure 9 shows the assembly process of the subassemblies.

The process of assembling the piston rod into the cylinder is analyzed to illustrate the performance of the proposed assembly method. As shown in Fig. 9I, the cylinder is fixed and is regarded as the base part. Initially, the piston rod is driven by the assembly force and gravity toward the cylinder. Once a collision is detected (Fig. 9I (a)), the contact force is calculated according to the penetration depth. Under the action of external forces and moments, the piston rod gradually moves

toward the final position. In Fig. 9I (b), the piston rod is in a state of non-equilibrium and will rotate. Then, by adjusting the attitude, the piston rod is assembled into the cylinder and is in a state of moment equilibrium (Fig. 9I (c)). Finally, the piston rod is driven mainly by gravity to move down. Once a certain position of the piston rod satisfies the assembly requirement, the assembly is completed (Fig. 9I (d)). The assembly process of the guide sleeve (see Fig. 9II) and the seal ring (see Fig. 9III) are similar to that of the piston rod. From Fig. 9, we know that the proposed method can not only position the virtual part accurately but also simulate the realistic assembly process.

Table 1 records the results of human factors evaluation during the assembly process of parts shown in Fig. 9. In Table 1, t denotes the assembly time. As can be seen from Table 1, as the assembling part gradually approached the final position, η increased gradually, indicating that as the assembling part was partially and gradually obscured by the assembled part, the positioning errors of assembling part caused by viewing perspective became greater and greater. When r and g varied within a certain range, λ_c was mainly affected by V (see Eq. (3)), so the visibility of assembly operation played a major role in assembly positioning. The hydraulic cylinder was easy and rapid to assemble, the energy expenditure of the operator can be neglected, so the fatigue factor almost had no effect on the assembly efficiency. When the assembling part was very close to its final position, although the viewing perspective and working comfort caused great uncertainties during the assembly process, the assembly time did not obviously increase, meaning that the final position of the assembling part was determined by the interactions of parts.

5 Real-world experiment validation and analysis

In order to validate that the proposed simulation method provides a realistic simulation and closely replicates a real-world assembly task, a series of real-world experiments were carried out to provide statistically significant results. The primary objective is to compare the assembly time and the results of human factor evaluation during the assembly process in a virtual environment with that of a similar real-world task. The comparison between real environment and virtual environment is trying to verify the feasibility of evaluating human factors under virtual environment and test whether the calculation of human factors based on virtual parts corresponds to that measured in real manual assembly operations. All users are mechanical engineering graduates, and they had knowledge of product assembly design. In addition, they were familiar with the proposed virtual assembly system. The following subsections describe the experiments in more detail.

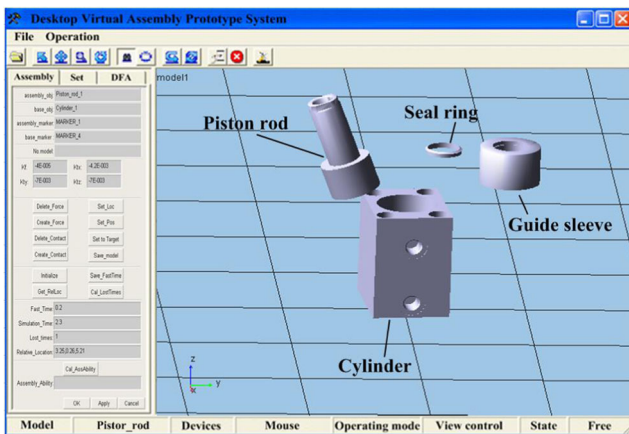


Fig. 8 A self-developed desktop virtual assembly system

Fig. 9 The assembly processes of subassemblies

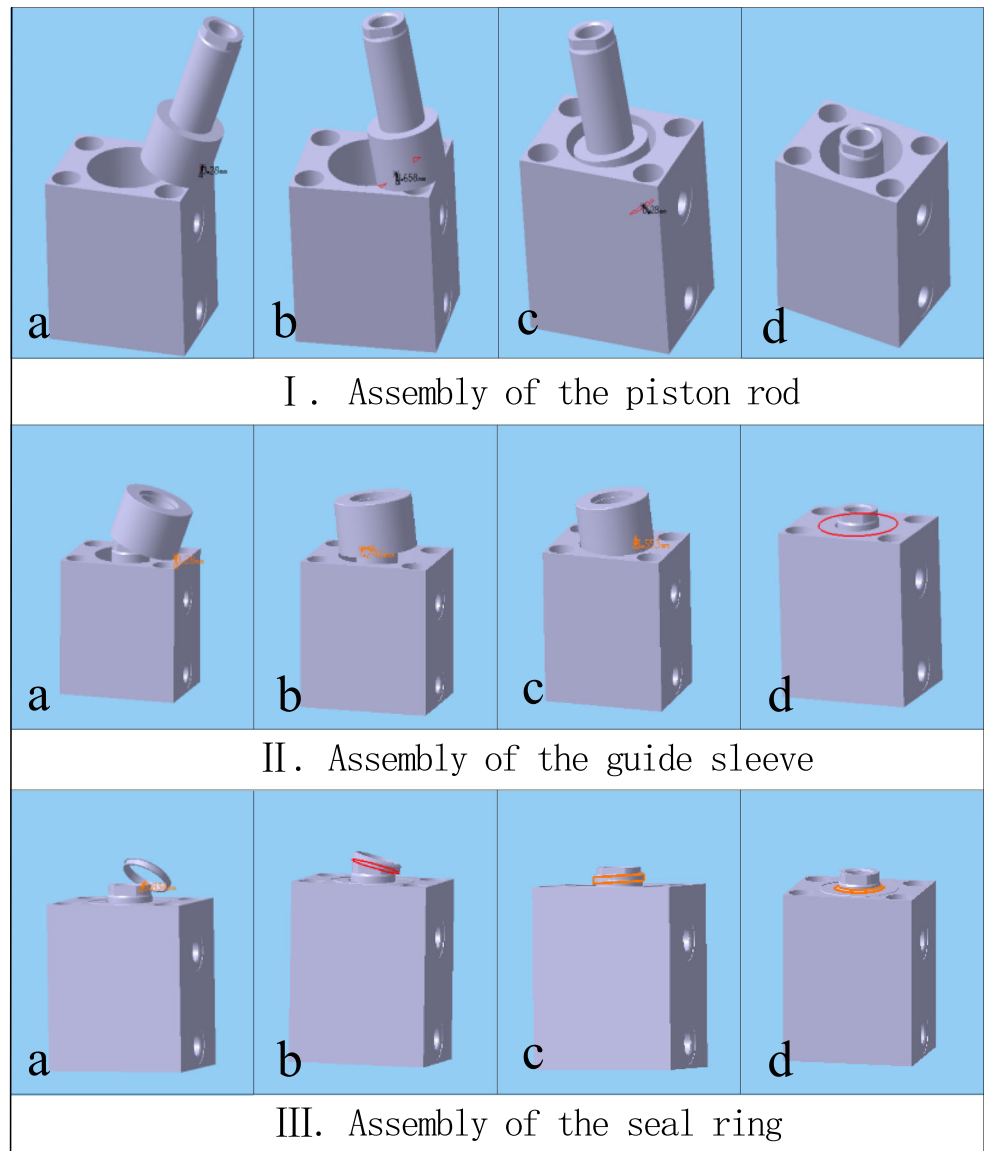


Table 1 The results of human factors evaluation during the assembly process of subassemblies shown in Fig. 9

		Visual factor			Comfort factor			Fatigue factor		
		<i>V</i>	<i>f</i>	η	<i>r</i>	<i>g</i>	λ_c	<i>t</i> (s)	<i>A</i> (kcal)	Ψ_c
I (piston rod)	a	1.00	0.95	0.05	0.90	1.00	0.05	1.40	1.80	0.99
	b	0.96	0.93	0.11	0.92	1.00	0.08	1.90	2.50	0.99
	c	0.40	0.88	0.65	0.88	1.00	0.62	2.50	3.20	0.98
	d	0.08	0.80	0.93	0.80	0.85	0.93	3.60	3.80	0.98
II (guide sleeve)	a	1.00	0.90	0.10	0.98	1.00	0.01	4.10	4.80	0.98
	b	1.00	0.90	0.10	0.98	1.00	0.01	4.90	5.10	0.98
	c	0.95	0.88	0.16	0.95	0.96	0.13	5.80	5.90	0.98
	d	0.10	0.82	0.91	0.85	0.90	0.92	6.50	6.30	0.97
III (seal ring)	a	0.95	0.92	0.12	1.00	0.95	0.07	6.90	6.70	0.97
	b	0.75	0.85	0.36	1.00	0.94	0.27	7.80	7.00	0.97
	c	0.52	0.80	0.58	0.95	0.90	0.52	8.50	7.40	0.97
	d	0.26	0.85	0.78	0.92	1.00	0.75	9.20	7.90	0.97

5.1 Real-world experiment set up

Figure 10 shows a participant undertaking the real-world task and the real-world experiment set-up. The geometric and physical parameters (e.g., mass, shape, size, and chamfer) of the real-world hydraulic cylinder model were fully consistent with that of the virtual model. In order to enhance the reliability of experimental results, the relative positions of all subassemblies at the beginning of each experiment in the real world were the same with that in the virtual environment. The real-world experimental environment comprises a camera and some sensors. In the real-world assembly operation, the sensors were mounted on certain parts of the operator's body (e.g., shoulders and center of body) and the assembling part to measure the real-time position parameters, and then the posture of the operator and the human factors could be determined mathematically by the methods proposed in Section 3. The specific calculation methods of human factors are as follows:

- V The camera recorded the assembly process and took photos at some given moments. Using the video or pictures to calculate the volume of visible and whole area of assembling part at different moments, then V was calculated by Eq.(1).
- f At first, at time i , the position of assembling part (denoted by P_i) was recorded by the sensor mounted on the center of assembling part. Thus, the motion direction of assembling part at time i was $P_i - P_{i-1} / |P_i - P_{i-1}|$. Then, the position of operator's eyes (denoted by P_{ie}) was recorded by the sensor mounted on operator's brow. Thus, the eye sight direction of operator was $P_i - P_{ie} / |P_i - P_{ie}|$. Finally, the angle between eye sight direction and motion direction was calculated and f was derived by the function shown in Fig. 3.
- r The positions of the operator's shoulders at time i (denoted by P_{irs} and P_{ils}) were recorded by the sensors mounted on them. Thus, the distance from the operator's shoulder to the assembling part was max

$(|P_{irs} - P_i|, |P_{ils} - P_i|)$ and r could be derived by the function shown in Fig. 4.

- g The position center of the operator's body (denoted by P_{ic}) was recorded by a sensor and the equation of plane of the operator's body was established according to P_{ic} , P_{irs} , and P_{ils} . Then, the angle between eyesight direction and plane of the operator's body was calculated and g was derived by the function shown in Fig. 5.

After V , f , r , and g were obtained, the vision influencing coefficient (η) and comfort coefficient (λ_c) were calculated by Eqs. 2 and 3, respectively.

There are three subtasks for the experimental validation. The first is assembly operation experiment for the comparison of assembly efficiency. The second is human factors evaluation experiment. The third is comparison and analysis of energy expenditure during assembly process.

5.2 Assembly operation experiment

In this experiment, three males and three females were selected to conduct both virtual assembly experiments and real assembly experiments. The positions of the operator and the assembly parts in the virtual environment were same with that in the real world. The virtual assembly was triggered by a click and the physical behavior of the operation was simulated automatically. The objective of this experiment is to investigate the correlation of virtual assembly and real assembly and the relationships between assembly performance and the complexity of assembly part by researching the change law of the assembly time for different assembly parts in virtual world and real world, respectively.

Giving the final product configuration scheme (see Fig. 9), which is a medium-scale hydraulic cylinder with four parts, each user performed assembly tasks in the proposed VR system and the real-world environment, respectively. Users assembled these parts according to the sequence shown in Fig. 9. The time taken to assemble the hydraulic cylinder in virtual environment was computed from the simulation. The time required for users to perform the first real assembly was recorded. Each real assembly task was performed ten times and the average taken. Figure 11 shows the results of time for assembly of hydraulic cylinder of each user under different situations.

As can be seen from Fig. 11, performing an assembly task in the virtual system almost takes the same time with that in the real world as a whole. Given the assembly process shown in Fig. 9, it indicates that the virtual assembly task is nearly consistent with the real task. However, there are some small differences between the real task and virtual task. The main reason is that the proposed VA method uses the Monte Carlo method to simulate the assembly process and it has a certain degree of uncertainty. In addition, during the virtual assembly

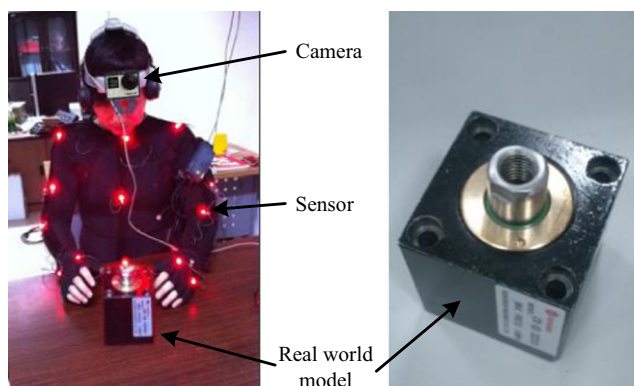
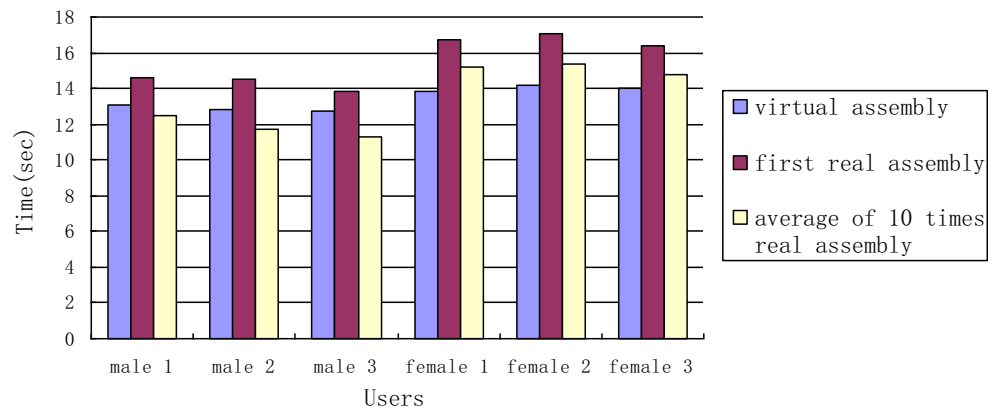


Fig. 10 Real-world experiment set up

Fig. 11 Time for assembly of hydraulic cylinder

process, some limited human factors (visual, comfort, and fatigue factors) are considered, while some other influencing factors (e.g., hands tremble and strength of operator) are neglected. For different operators, both men and women, the time of virtual assembly task has little change. The virtual assembly time of males is slightly less than that of females; this is because compared with females, the arm of males is longer and the height is higher, which improve the visual condition and work posture (see Section 3), and then increase the assembly efficiency.

The real assembly time of males is generally less than that of females, indicating that the strength of the operator has a significant influence on the assembly task for a heavier object, such as the hydraulic cylinder (see Fig. 10) with a weight of 10 kg. For all operators, the average time of 10 times real assembly is clearly less than the first real assembly time and the virtual assembly time, this can be attributed to an “adapting process.” The multiple and repetitive operations could improve manual performance in real-world tasks given an ordered procedure. Furthermore, the virtual task is performed little faster than the first real task. Through interviews it was found that manipulating the heavier objects and positioning them accurately for the first time felt “unfamiliar,” which would increase the difficulty of manual operations and the randomness of assembly positioning.

In order to investigate the influences of complexity and weight of parts on assembly performance, the time taken to assemble the subassemblies in virtual environment was computed from the simulation. Each real subassembly was assembled ten times and the average assembly time of males and females were taken, respectively. Figure 12 shows the results.

It can be seen that with the decrease of mass and size of assembly part, the difficulty to grab, move, and position the part decreased; no matter the real task or the virtual task, the assembly time decreased, which means that the assembly time was determined by the complexity and weight of assembly part to some extent. When the users had been familiar with the real assembly process gradually, the adapting process made the real task performed by males faster than the virtual

task, while the real task performed by females still slower than the virtual task. These results clearly show that in the real task, when the strength of operator is relatively small and the manipulated part is relatively heavy, the assembly task was time consuming. Although the proposed assembly method does not take into account the strength of the operator, it still reflects the general real assembly process. The proposed VA system has almost the same efficiency as the real-world task and provides a realistic and intuitive assembly process simulation in virtual space.

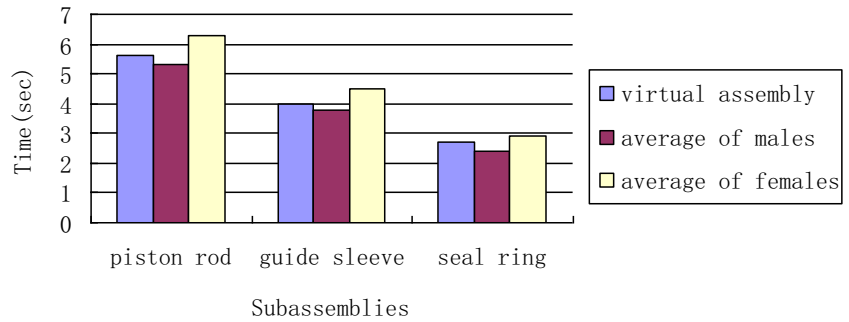
5.3 Human factors evaluation experiment

In this experiment, users were separated into three groups. Each group had five users. Group 1 were asked to conduct the virtual assembly experiment, while groups 2 and 3 were asked to conduct the real-world experiment. During the real-world assembly task, the operating conditions of each user in group 2 were very good. They can adjust their position and posture freely to select any comfortable operating posture in real time, according to the physical attributes (eg. mass, shape and size) and spatial position of assembling part. While the users in group 3 had to face poor working conditions, they were asked to stand away from the assembling part and the assembling part was partially or wholly obscured due to the viewing perspective, the assembly difficulty was increased artificially.

As we measured in Section 5.2, the time of assembling the hydraulic cylinder was about 16 s. During the assembly process, we selected some different instants t_i ($t_i=3$ s, 6 s, ..., 15 s) and calculated the vision influencing coefficient and comfort coefficient of each group at t_i . Figures 13 and 14 shows the results of visual factor and comfort factor evaluation under different assembly environments, respectively.

After all users performing the same assembly tasks in virtual and real environment, the main findings of the study were as follows: At each instant, the evaluation values of human factors of group 1 were between that of groups 2 and 3. This is because during the assembly process, group 1 used the virtual

Fig. 12 Time of assembling subassemblies



model to simulate the assembly process and evaluate the human factors, which represented the general working conditions. While groups 2 and 3 represented the best and worst working conditions, respectively. The evaluation values of human factors recorded by group 2 were minimum, which means that for the assembly operation with good view and operability, it would reduce the operating errors and improve the accuracy and efficiency of assembly positioning. The change law of each curve in Figs. 13 and 14 was similar, indicating that the assembly process in virtual system corresponded to that in real manual assembly environment. The proposed methods can realistically simulate the assembly process and accurately evaluate the human factors during assembly process.

5.4 Fatigue evaluation experiment

In this experiment, users were separated into two groups. Each group had five users. Groups 1 and 2 conducted the virtual assembly experiment and real-world experiment, respectively, in order to test whether the real fatigue process conforms the theoretical prediction in virtual environment. All users were asked to conduct the assembly work in a continuous operation for 1 h. The working time was divided into four time segments and each time segment had 15 min. The time of virtual

assembly task was computed from the simulation. The time of real assembly task was the time required for users to perform the manual operation. Within each time segment, the average time and assembly success rate of assembling the hydraulic cylinder of each user were computed and the average of each group was taken (see Figs. 15 and 16). The average assembly time and success rate can be regarded as the indicators to analyze the efficiency and performance of assembly [14]. From [14], the assembly success rate (ASR) is defined as the ratio of the successful number of assemblies to the total number of assemblies, which indicates the success probability of assembly tasks.

As we can see from Fig. 15, in general, the average time to complete assembly tasks increased with the increase of working time, indicating that the energy expenditure greatly impact the assembly efficiency. Compared with virtual assembly, the growth of real assembly time was slower. In the first two time segments, the average time of virtual task was less than that of real task. However, in the last two time segments, the real task was more efficient and required less assembly time. After assessing participant feedback and further study of the experimental process, it was realized that the slowing growth of real assembly time might be attributed to the adapting process. In the real-world experiment, although the energy expenditure would increase the assembly time, the operator became

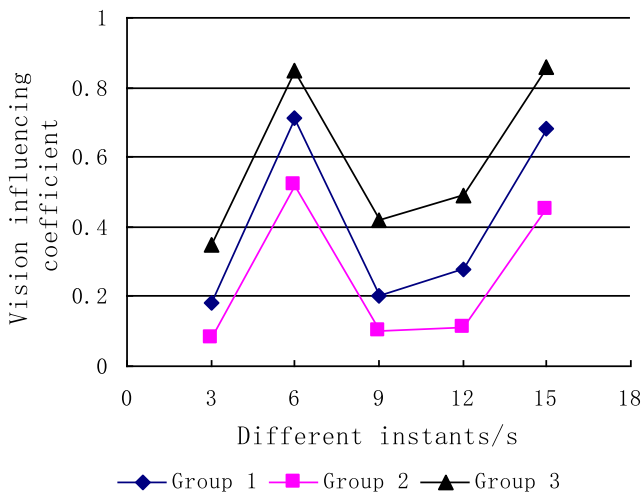


Fig. 13 Results of visual factor evaluation

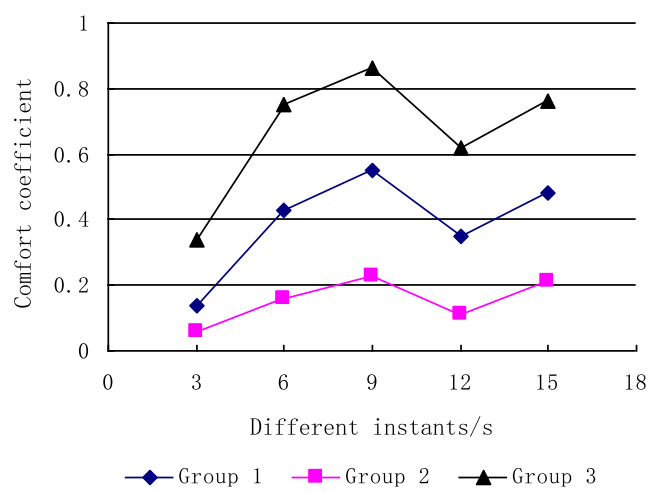


Fig. 14 Results of comfort factor evaluation

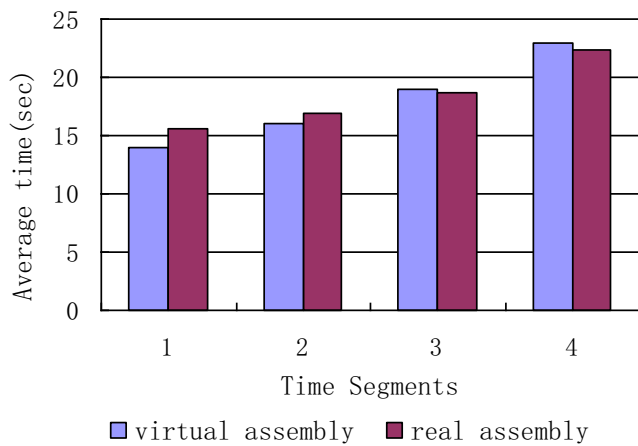


Fig. 15 The average assembly time within each time segment

accustomed to the assembly task and more familiar with assembly process by exploring the rules of assembly operation, which would save the assembly time to a certain extent. When the operators continuously worked more than 30 min, they showed more confidence during the assembly process. This was verified through observation and video evidence. While the virtual task was conducted automatically and the energy expenditure was computed theoretically during the assembly process, thus the growth of assembly time was relatively stable.

As can be seen from Fig. 16, the increase of working time resulted in the decrease of ASR of the assembly tasks. This is because the energy expenditure of operators made it difficult to manage the assembling part and increased the uncertainties of assembly operations, which further reduced the accuracy of part positioning. Within the first time segment, ASR was relatively high and approximated to 100 %, which means that the energy consumption had little effect on the positioning of parts, and the positioning errors can hardly lead to the failure of tasks. When the assembly operation lasted for 1 h, ASR decreased from 0.96 to 0.75 (dropped by 21.8 %) in the virtual environment, while decreased from 0.92 to 0.68 (dropped by

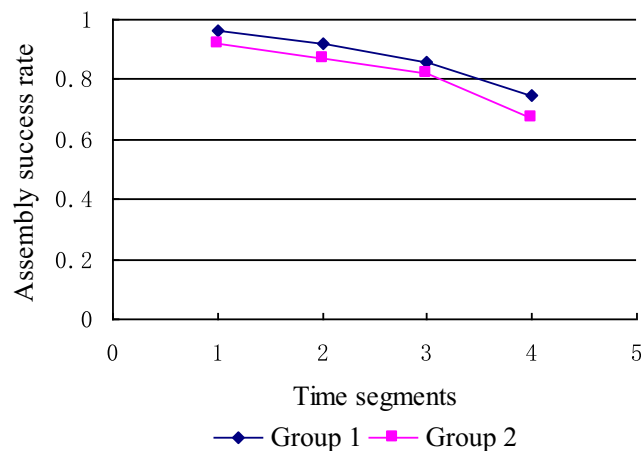


Fig. 16 The assembly success rate within each time segment

26.1 %) in the real-world environment, indicating that the parts were hard to be assembled due to energy consumption and the real energy consumption process was almost consistent with the theoretical calculation in the virtual environment. This result was predictable given the randomness of direction of assembly force due to the energy consumption of operators (see Section 3.3).

Overall, these results show that the fatigue increases the difficulty of assembly tasks and reduces the working efficiency. For the operator with enough energy, it is easy and rapid to perform the assembly tasks. Otherwise, it is time consuming and easy to fail.

6 Conclusions and future work

The human factors calculation and assembly process simulation method presented in this paper is mainly based on our previously presented physics-based assembly method, in which the assembling part is guided by the assembly force and the physics of the interaction is simulated. In this study, the human factors involved in the assembly process, including the visibility of an assembling part, posture, reachability, and fatigue of an operator, are quantified for each operation, and assembly operations are simulated in a virtual environment. The new calculation methods of the estimated final position and the assembly force are presented to perform a more realistic assembly operation. The assembly force is categorized into two types: exerted on freely moving parts and exerted on colliding parts, and the calculation methods of these two forces are presented. A self-developed desktop virtual design platform has been developed and a case study is used to verify the performance and capabilities of the simulation method. A series of real-world experiments were carried out and the assembly time and the results of human factors evaluation during the assembly process in a virtual environment with that of a similar real-world task were compared. The comparison between real environment and virtual environment verified the feasibility of evaluating human factors under virtual environment and validated the calculation of human factors based on virtual parts corresponds to that measured in real manual assembly operations.

On the basis of this work, our next research will focus on more statistical analysis of the effects of more factors (such as the assembly proficiency, working conditions, and grasping difficulty) on the performance and results of the assembly tasks, and improve the calculation methods of the human factors to make the virtual assembly simulations more consistent with the real world.

Acknowledgments The authors wish to thank the anonymous reviewers for their helpful comments on this paper. The Project Supported by Natural Science Basic Research Plan in Shaanxi Province of China (Program No. 2014JZ016).

References

1. George C, Dimitris M, Dimitris F (2000) A virtual reality-based experimentation environment for the verification of human-related factors in assembly processes. *Robot Comput Integr Manuf* 16(4): 267–276
2. Judy MV, Georges D (2011) A conceptual framework to support natural interaction for virtual assembly tasks. Proceedings of the ASME World Conference on Innovative Virtual Reality (WINVR2011), Milan, Italy, pp 27–29
3. Loic T, Georges D, Jerome P (2010) Interactive simulation of CAD models assemblies using virtual constraint guidance. *Int J Interact Des Manuf* 4(2):95–102
4. Christian D, Jungwon Y (2011) Assembly simulations in virtual environments with optimized haptic path and sequence. *Robot Comput Integr Manuf* 27(2):306–317
5. Loic T, Georges D, Jerome P (2010) Haptic assembly of CAD models using virtual constraint guidance. Proceedings of the ASME 2010 World Conference on Innovative Virtual Reality, Ames, Iowa, USA
6. Liu ZY, Tan JR (2007) Constrained behavior manipulation for interactive assembly in a virtual environment. *Int J Adv Manuf Technol* 32(7):797–810
7. Yang RD, Fan XM, Wu DL, Yan JQ (2007) Virtual assembly technologies based on constraint and DOF analysis. *Robot Comput Integr Manuf* 23(4):447–456
8. Frohlich B, Tramberend H, Beers A, Agarawala M, Baraff D (2000) Physically-based manipulation on the responsive workbench. Proceedings of the IEEE Virtual Reality Conference, New Brunswick, NJ, USA, pp 5–11
9. Germanico GB, Hugo M, Theodore L, James R, Samir G (2014) The development of a physics and constraint based haptic virtual assembly system. *Assem Autom* 34(1):41–55
10. Look A, Schomer E (2001) Physically based cables for assembly simulation in virtual reality. 13th European Simulation Symposium, Ghent, Belgium, pp 294–297
11. Abhishek S, Judy MV, James HO (2007) Combining geometric constraints with physics modeling for virtual assembly using SHARP. In: ASME design engineering technical conferences and computers and information in engineering conference, Las Vegas, NV, USA
12. Abhishek S, Judy MV, James HO (2010) Combining dynamic modeling with geometric constraint management to support low clearance virtual manual assembly. *J Mech Des* 132(8):1002–1008
13. Holt POB, Ritchie JM, Day PN, Simmons JEL, Robinson G, Russell GT, Ng FM (2004) Immersive virtual reality in cable and pipe routing: design metaphors and cognitive ergonomics. *J Comput Inf Sci Eng* 4(3):161–170
14. Gao W, Shao XD, Liu HL (2014) Virtual assembly planning and assembly-oriented quantitative evaluation of product assemblability. *Int J Adv Manuf Technol* 71(1):486–496
15. Jayaram S, Wang Y, Tirumali H, Lyons K, Hart P, Jayaram U (1999) VADE: a virtual assembly design environment. *IEEE Comput Graph Appl* 19(6):44–50
16. Sankar J, Hugh IC, Kevin WL (1997) Virtual assembly using virtual reality techniques. *Comput Aided Des* 29(8):575–584
17. Wan HG, Gao SM, Peng QS, Dai GZ, Zhang FJ (2004) MIVAS: A multi-modal immersive virtual assembly system. ASME International Design Engineering Technical Conferences (DETC 2004) and Computers and Information in Engineering Conference, Salt Lake City, UT, USA, pp 113–122
18. Luis M, Norman M, Terrence F (2003) A constraint manager to support virtual maintainability. *Comput Graph* 27(1):19–26
19. Wang QH, Li JR, Gong HQ (2006) A CAD-linked virtual assembly environment. *Int J Prod Res* 44(3):467–486
20. Zhong YM, Wolfgang MW, Ma WY (2002) Incorporating constraints into a virtual reality environment for intuitive and precise solid modeling. Proceedings of the sixth international conference on information visualization, London, England
21. Zhang SY, Gao Z, Tan JR (2002) Research of movement navigation based on assembly constraint recognition. *Chin J Mech Eng* 15(1): 6–10
22. Wang Y, Jayaram U, Jayaram S, Imtiyaz S (2003) Methods and algorithms for constraint-based virtual assembly. *Virtual Reality* 6(4):229–243
23. Gupta R, Whitney D, Zeltzer D (1997) Prototyping and design for assembly analysis using multimodal virtual environments. *Comput Aided Des* 29(8):585–597
24. Adam SC, Scott DM, Bert B (2001) A haptic assembly and disassembly simulation environment and associated computational load optimization techniques. *J Comput Inf Sci Eng* 1(2):113–122
25. Adam SC, Bert B (2002) Collision detection for virtual objects in a haptic assembly and disassembly simulation environment. ASME Design Engineering Technical Conferences and Computers and Information in Engineering Conference, Montreal, Canada
26. Samir G, Ulises ZC (2007) The effect of contact force sensations on user performance in virtual assembly tasks. *Virtual Reality* 11(4): 287–299
27. Samir G, Ulises ZC (2009) Modeling dynamic behavior of parts in virtual assembly environment. Proceedings of the World Conference on Innovative Virtual Reality, Chalon sur Saone, France
28. Chang EK, Judy MV (2004) Collision detection and part interaction modeling to facilitate immersive virtual assembly methods. *J Comput Inf Sci Eng* 4(2):83–90
29. Wang Y, Jayaram U, Jayaram S, Lyons K (2001) Physically based modeling in virtual assembly. ASME Design Engineering Technical Conferences and Computers and Information in Engineering Conference, Pittsburgh, pp 295–305
30. Lim T, Ritchie JM, Corney JR, Dewar RG, Schmidt K, Bergsteiner K (2007) Assessment of a haptic virtual assembly system that uses physics-based interactions. IEEE International Symposium on Assembly and Manufacturing, Ann Arbor, Michigan, USA, pp 147–153
31. Brad MH, Judy MV (2007) Desktop haptic virtual assembly using physically based modeling. *Virtual Reality* 11(4):207–215
32. Abhishek S, Su HJ, Judy MV (2006) SHARP: a system for haptic assembly & realistic prototyping. In: ASME design engineering technical conferences and computers and information in engineering conference, Philadelphia, PA, USA
33. William AM, Kevin DP, James JT (1999) Six degree-of-freedom haptic rendering using voxel sampling. Proceedings of the SIGGRAPH 99 Conference, Annual Conference Series, Los Angeles, CA, USA
34. Just C, Bierbaum A, Baker A, Cruz-Neira C (1998) VR juggler: a framework for virtual reality development. In: 2nd Immersive projection technology workshop (IPT98), CD-ROM. Ames, IA
35. Lin MC (2008) Haptic rendering: foundations, algorithms and applications. A.K. Peters publishers
36. Atsuko E, Noriaki Y, Tatsuya S (2013) Automatic estimation of the ergonomics parameters of assembly operations. *CIRP Ann Manuf Technol* 62(1):13–16
37. Yang RD, Fan XM, Wu DL, Yan JQ (2007) A virtual reality-based experiment environment for engine assembly line workplace planning and ergonomics evaluation. *Lecture Notes in Computer Science* 4563:594–603